

# NMR Studies on Conformational and *N*-Configurational Interconversion in 3-Methyl Derivatives of the Non-Narcotic Analgesic Drug Nefopam

Robert Glaser\* and Jeanine Blumenfeld

Department of Chemistry, Ben-Gurion University of the Negev, Beer-Sheva 84105, Israel

Shimona Geresh

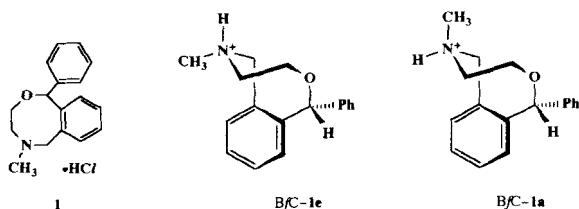
Institutes of Applied Research, Ben-Gurion University of the Negev, Beer-Sheva 84110, Israel

Two different *N*-configurations and two different eight-membered ring conformations were found in the diastereomeric crystalline (1*R*,3*S*)/(1*S*,3*R*)- and (1*R*,3*R*)/(1*S*,3*S*)-3-methylnefopam hydrochloride salts. <sup>1</sup>H and <sup>13</sup>C NMR spectroscopy showed that both crystalline epimers undergo *N*-configurational and eight-membered ring conformational equilibria on dissolution in a solvent (e.g. CD<sub>2</sub>Cl<sub>2</sub>). Observation of *N*-H proton vicinal coupling in both the solution-state major and minor species for each epimer signifies slow exchange limit kinetic regimes for *N*-configurational interconversion via a prototropic shift-nitrogen inversion. Since previous studies have shown 2,5-benzoxazocine ring inversion to be unfavourable, the finding of weighted time-average vicinal coupling constants for the —OCH(CH<sub>3</sub>)CH<sub>2</sub>NH(CH<sub>3</sub>)CH<sub>2</sub>— moiety is interpreted in terms of a fast exchange limit (and in some cases fast magnetic site exchange broadening) kinetic regime for eight-membered ring conformational change. For each C-3 epimer; a quantitative estimation was made for the 2<sup>n</sup> = 4 solution-state diastereomeric forms resulting from the two stereogenic elements of *N*-configuration and ring conformation. Comparisons were made with the parent nefopam hydrochloride, *N*-desmethylnefopam hydrochloride metabolite and the nefopam methiodide quaternary ammonium salt.

KEY WORDS Nefopam Analgesic Benzoxazocine Conformation Stereochemistry <sup>1</sup>H NMR <sup>13</sup>C NMR <sup>1</sup>H-<sup>1</sup>H coupling constants

## INTRODUCTION

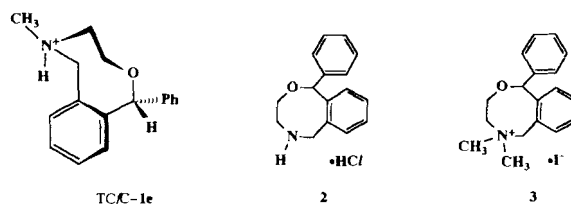
Nefopam hydrochloride [(±)-5-methyl-1-phenyl-3,4,5,6-tetrahydro-1*H*-2,5-benzoxazocine hydrochloride (**1**)] is a non-narcotic analgesic drug.<sup>1,2</sup> X-ray crystallographic determination of the structures of (+)-<sup>3</sup> and (–)-chiral crystals<sup>4</sup> and of the racemic modification<sup>3</sup> of crystalline nefopam · HCl (**1**) show the 2,5-benzoxazocine ring to be bent into the boat-(flattened chair) conformation (BfC). In this geometry, the phenyl ring is in an *exo* position, while the *N*-methyl group is equatorially oriented (see structure BfC-1e).<sup>3</sup>



<sup>1</sup>H and <sup>13</sup>C NMR spectroscopy [CD<sub>2</sub>Cl<sub>2</sub> or acidic aqueous solutions of either (+)- or (±)-crystals] shows the presence of axial (a) and equatorial (e) *N*-methyl BfC diastereomers (BfC-1a,e) in a ca. 3:2 ratio.<sup>3a,5</sup>

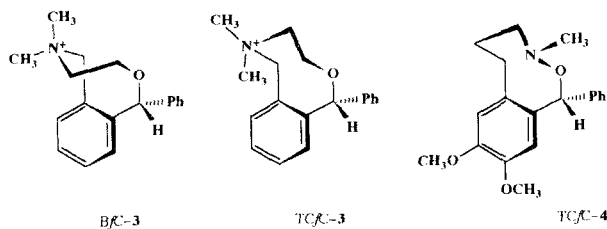
\* Author to whom correspondence should be addressed.

Diastereomerizations via epimerization at the chirotopic and labile stereogenic<sup>6</sup> nitrogen of amine salts are well known,<sup>7</sup> and arise from a prototropic shift/nitrogen inversion. Solution-state BfC-conformational and *N*-configurational assignments were made using NMR techniques.<sup>3,5</sup> Line broadening in <sup>1</sup>H NMR resonances from the equatorial species (BfC-1e) testifies to the presence of a third species.<sup>3a,5</sup> However, reduced temperature resulted only in line sharpening for BfC-1e, suggesting a low concentration hidden partner for the third species.<sup>3a,5</sup> Molecular mechanics exploration of other benzoxazocine ring conformational models showed the twist-chair-(flattened chair) conformation (TCfC-1e) to be very close in energy to that of BfC-1e.<sup>3b</sup>

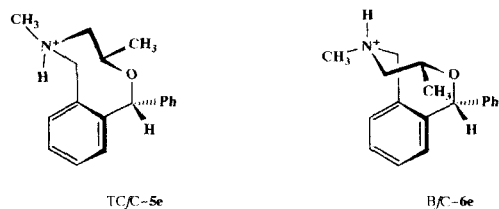


Broadened NMR resonances were seen for nefopam derivatives containing two internally diastereotopic *N*-substituents [e.g. the *N*-desmethylnefopam hydrochloride<sup>8</sup> (**2**) metabolite and nefopam methiodide<sup>9</sup>

(3)]. This was interpreted as arising from a rapid equilibration between different eight-membered ring conformations,<sup>8,9</sup> since previous studies<sup>3b</sup> showed ring inversion for nefopam to be sterically (and hence energetically) unfavourable. Time-averaged  $^3J(\text{HH})$  vicinal coupling constants pointed to a clear preponderance for the solution-state *BfC*-3 conformation of the quaternary ammonium salt (3).<sup>9</sup> Direct observation of the *TCfC* conformation for the nefopam 2,5-benzoxazocine ring was forthcoming from the x-ray crystallographically determined structure of crystalline nefopam methiodide.<sup>10</sup> Conformational disorder was observed for the crystal, and occupancies of the *BfC*-3 and *TCfC*-3 conformations were respectively 56(1):44(1) at 298 K.<sup>10</sup> For the same data crystal the *BfC*-3:*TCfC*-3 conformational ratio was 61(1):39(1) at  $-80^\circ\text{C}$ .<sup>11</sup>



Inspection of the literature showed a *TCfC* conformation for the ( $\pm$ )-8,9-dimethoxy-3-methyl-1-phenyl-3,4,5,6-tetrahydro-1*H*-2,3-benzoxazocine free base (*TCfC*-4).<sup>12</sup> The phenyl ring occupies a similar *exo* orientation on the 2,3- and 2,5-benzoxazocine rings as shown by x-ray determined structures for 1-4.<sup>3a,b,8,10,12</sup> These studies also show the same eight-membered ring flattened-region occupancy by the  $-\text{OCH}(\text{Ph})-\text{o}-\text{C}_6\text{H}_4-$  fragment, while *BfC*-3 and *TCfC*-3 conformations of the quaternary ammonium salt differ in the arrangement of fragment  $-\text{N}(\text{CH}_3)_2\text{CH}_2\text{CH}_2-$ .<sup>3a,b,8,10</sup> Preliminary molecular mechanics calculations suggested that appropriate *C*-methyl substitution of the nefopam 2,5-benzoxazocine ring could result in stabilization of the *TCfC* conformation. Recently, we reported the single-crystal x-ray crystallographic determination of solid-state conformations for epimeric *C*-methyl *cis*- and *trans*-to-phenyl analogues of nefopam.<sup>15</sup> Crystalline (1*R*,3*S*,5*R*)/(1*S*,3*R*,5*S*)-3-methylnefopam  $\cdot$  HCl (5) and (1*R*,3*R*,5*R*)/(1*S*,3*S*,5*S*)-3-methylnefopam  $\cdot$  HCl (6) were found in the respective *TCfC*-5*e* and *BfC*-6*e* conformations, as expected.<sup>15</sup> The configuration at the stereolabile nitrogen is also different in the two solid-state structures [both *C*- and *N*-methyl groups are *cis*-to-phenyl in *TCfC*-5*e*, whereas both are *trans*-to-phenyl in *BfC*-6*e*].<sup>15</sup>

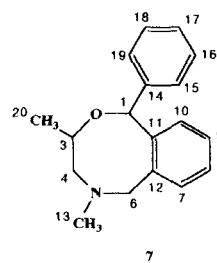


This paper reports conformational and *N*-configurational interconversion for each of the two *C*-methyl nefopam derivatives in the solution state.

## RESULTS AND DISCUSSION

### NMR studies

$^1\text{H}$  NMR spectroscopy showed that a *ca.* 2:1 mixture of the respective (1*R*,3*S*)/(1*S*,3*R*)- and (1*R*,3*R*)/(1*S*,3*S*)-3-methylnefopam free base diastereomers were formed in the cyclization reaction crude product. Major and minor species (*ca.* 7:6 for 5 and *ca.* 3:2 for 6) were found by  $^1\text{H}$  and  $^{13}\text{C}$  NMR spectroscopy on dissolution of the corresponding HCl salts in  $\text{CD}_2\text{Cl}_2$ . Sharp spectral lines were noted for the major and minor components of 5 and for the major species of 6. However, severe line broadening of ambient temperature H-31,41, 42,61 absorbances from the minor 6 constituent testified to a dynamic equilibrium involving another species. Reduction of the probe temperature to 230 K resulted in considerable sharpening of these lines.  $^1\text{H}$  and  $^{13}\text{C}$  NMR spectral parameters for the major/minor 5 and 6 solution-state species versus those from the parent (1*R*,5*R*)/(1*S*,5*S*)-nefopam  $\cdot$  HCl salt (1) are reported in Table 1 together with data from (1*R*)/(1*S*)-*N*-desmethylnefopam  $\cdot$  HCl (2) and (1*R*)/(1*S*)-nefopam methiodide (3). Homonuclear decoupling was used to ascertain  $^1\text{H}$ - $^1\text{H}$  coupling networks in each species.  $^{13}\text{C}$  NMR absorbance multiplicities for 5 and 6 were determined using DEPT pulse sequence spectra ( $90^\circ$  and  $135^\circ$  pulse angles) in comparison with the corresponding  $^{13}\text{C}\{^1\text{H}\}$  NMR spectra. Structure 7 is the numbering diagram for carbons in 5 and 6 (descriptors for geminal protons are given using crystallographic notation where H-41,42 designate protons bonded to C-4).



Coupling constants and chemical shifts involving the three protons of the  $\text{C}(3)\text{H}-\text{C}(4)\text{H}_2$  fragment in 5 and 6 were calculated<sup>16</sup> using *ab1* and *ab2* subspectra from the eight-line AB portion of the reduced ABX system upon {*N*-H}. The H-41,42 diastereotopic geminal protons were assigned antiperiplanar-like or synclinal (*gauche*)-type relationships relative to H-3 on the basis of the respective vicinal coupling constant magnitude [the larger of the two  $^3J(3,41)$  and  $^3J(3,42)$  values is approximately three times that of the other]. Diastereotopic H-61,62 protons reside in very different magnetic environments, as evidenced by their relatively large chemical shift differences. The higher field absorbance was assigned as the *anti*-to-oxygen H-62 by analogy with  $^1\text{H}$  NMR spectra of *BfC*-1*a,e* and other 2,5-benzoxazocines.<sup>3a,5,8-10</sup> Similarly to the case of *BfC*-1*a*, this assignment was confirmed by the finding of 1.5% and 2.5% nuclear Overhauser effect (NOE) intensity enhancements to the major and minor aromatic-H-7 absorbances upon {H-62 of the respective 5 or 6

**Table 1.** Aliphatic  $^1\text{H}$  and  $^{13}\text{C}$  NMR spectral parameters for (1*R*,3*S*,5*S*)/(1*S*,3*R*,5*R*)- and (1*R*,3*S*,5*R*)/(1*S*,3*R*,5*S*)- *N*-methyl diastereomeric 3-methylnepfopam hydrochloride salt mixture (5) and (1*R*,3*R*,5*S*)/(1*S*,3*S*,5*R*)- and (1*R*,3*R*,5*R*)/(1*S*,3*S*,5*S*)-3-methylnepfopam hydrochloride salt mixture (6), versus (1*R*,5*S*)/(1*S*,5*R*)- and (1*R*,5*R*)/(1*S*,5*S*)-nepfopam hydrochloride salt mixture (1), (1*R*)/(1*S*)-*N*-desmethylnepfopam hydrochloride (2) and (1*R*)/(1*S*)-nepfopam methiodide (3)<sup>a</sup>

	1 <i>R</i> ,3 <i>S</i> ,5 <i>S</i> / 1 <i>S</i> ,3 <i>R</i> ,5 <i>R</i> - Major isomer (5) <sup>b</sup>	1 <i>R</i> ,3 <i>S</i> ,5 <i>R</i> / 1 <i>S</i> ,3 <i>R</i> ,5 <i>S</i> - Minor isomer (5) <sup>b</sup>	1 <i>R</i> ,3 <i>R</i> ,5 <i>S</i> / 1 <i>S</i> ,3 <i>S</i> ,5 <i>R</i> - Major isomer (6) <sup>c</sup>		1 <i>R</i> ,3 <i>R</i> ,5 <i>R</i> - 1 <i>S</i> ,3 <i>S</i> ,5 <i>S</i> - Minor isomer (6) <sup>c</sup>		1 <i>R</i> ,5 <i>S</i> / 1 <i>S</i> ,5 <i>R</i> - Major isomer (1) <sup>d</sup>		1 <i>R</i> ,5 <i>R</i> / 1 <i>S</i> ,5 <i>S</i> - Minor isomer (1) <sup>d</sup>	1 <i>R</i> :1 <i>S</i> - (2) <sup>e</sup>	1 <i>R</i> :1 <i>S</i> - (3) <sup>f</sup>
$\delta_{\text{H}}$ (ppm)											
H-1	5.82	5.89	5.98	[5.94]	5.94	[5.90]	5.78	5.73	5.76	5.80	
H-31	—	—	4.70	[4.72]	<sup>g</sup>	[4.88]	4.49	4.73	4.48	4.63	
H-32	4.14	4.33	—	—	—	—	4.10	3.98	4.04	4.11	
H-41	2.93	3.32	2.96	[~2.9]	<sup>g</sup>	[~2.9]	3.29	2.96	3.19	3.27	
H-42	3.30	2.82	2.76	[~2.9]	<sup>g</sup>	[~2.9]	2.81	3.13	3.19	3.98	
H-51	13.07	—	—	—	13.20	[12.35]	—	13.55	10.34	—	
H-52	—	12.60	12.76	[12.01]	—	—	13.08	—	9.89	—	
H-61	5.61	5.15	4.92	[4.99]	<sup>g</sup>	[6.05]	5.00	5.92	5.26	5.81	
H-62	4.05	4.13	4.39	[4.36]	3.84	[3.91]	4.41	3.91	4.39	4.72	
H-7	7.32	7.58	<sup>h</sup>	—	<sup>h</sup>	—	7.65	<sup>h</sup>	7.53	<sup>h</sup>	
H-131	—	2.94	2.99	[3.02]	—	—	2.97	—	—	3.73	
H-132	2.56	—	—	—	2.65	[2.67]	—	2.64	—	3.40	
H-201	1.50	1.37	—	—	—	—	—	—	—	—	
H-202	—	—	1.44	[1.41]	1.41	[1.38]	—	—	—	—	
$J(\text{H,H})$ (Hz)											
31,20	—	—	6.5 (1)	[6.5 (1)]	6.5 (1)	[6.7 (1)]	—	—	—	—	
32,20	6.6 (1)	6.5 (1)	—	—	—	—	—	—	—	—	
31,32	—	—	—	—	—	—	-13.8 (2)	-13.8 (3)	-13.2 (2)	-14.5 (1)	
31,41	—	—	12.1 (3)	[11.8 (5)]	<sup>g</sup>	[~10.8]	12.0 (2)	10.8 (3)	8.1 (2)	12.8 (1)	
31,42	—	—	4.6 (2)	[3.5 (5)]	<sup>g</sup>	—	4.3 (3)	3.2 (3)	5.1 (2)	3.8 (1)	
32,41	2.3 (1)	2.2 (1)	—	—	—	—	4.8 (2)	3.4 (3)	3.9 (1)	4.3 (2)	
32,42	6.6 (1)	8.5 (1)	—	—	—	—	2.2 (3)	3.0 (2)	3.9 (1)	<1	
41,42	-14.0 (1)	-13.1 (1)	-14.4 (3)	—	<sup>g</sup>	—	-14.3 (3)	-13.9 (2)	—	-14.0 (2)	
41,51	4.8 (4)	—	—	—	<sup>g</sup>	—	—	7.7 (2)	—	—	
42,51	3.5 (1)	—	—	—	<sup>g</sup>	—	—	2.7 (3)	—	—	
51,13	5.0 (1)	—	—	—	4.9 (1)	[4.8 (1)]	—	5.0 (1)	—	—	
51,61	1.5 (1)	—	—	—	<sup>g</sup>	[3.0 (2)]	—	2.9	3.3 (2)	—	
51,62	3.4 (1)	—	—	—	<sup>g</sup>	[<1]	—	<1	2.6 (5)	—	
41,52	—	3.2 (1)	2.1 (3)	—	—	—	2.4 (2)	—	—	—	
42,52	—	7.9 (2)	2.7 (2)	—	—	—	3.5 (3)	—	—	—	
52,13	—	4.9 (1)	4.9 (1)	[4.9 (1)]	—	—	5.0 (1)	—	—	—	
52,61	—	7.2 (1)	7.8 (3)	[8.3 (1)]	—	—	7.7 (1)	—	8.9 (4)	—	
52,62	—	<1	5.1 (1)	[4.9 (2)]	—	—	4.5 (2)	—	3.9 (5)	—	
61,62	-13.3 (1)	-12.7 (1)	-11.6 (1)	[-11.6 (2)]	-12.9 (1)	[-13.0 (1)]	-11.8 (2)	-12.9 (4)	-12.3 (3)	-12.4 (1)	
$\delta_{\text{C}}$											
C-1	84.83	83.95	77.63	—	77.32	—	86.06	85.45	85.77	86.51	
C-3	70.39	70.46	68.11	—	70.20	—	64.60	65.93	66.93	65.61	
C-4	57.70	60.57	52.55	—	<sup>g</sup>	—	48.57	51.06	42.48	58.20	
C-6	56.04	58.54	57.70	—	56.42	—	58.13	56.69	48.65	68.09	
C-131	—	45.74	40.08	—	—	—	40.23	—	—	51.12	
C-132	40.78	—	—	—	42.20	—	—	41.30	—	53.20	
C-201	20.21	20.43	—	—	—	—	—	—	—	—	
C-202	—	—	16.40	—	16.75	—	—	—	—	—	

<sup>a</sup> In ppm downfield from tetramethylsilane, 300 MHz (for  $^1\text{H}$ ), 75 MHz (for  $^{13}\text{C}$ ).  $\text{CD}_2\text{Cl}_2$ , 298 K [230 K values in square brackets, 400 MHz], estimated standard deviations (esd) for last digit of  $J$ -value in parentheses.

<sup>b</sup> Major : minor ratio *ca.* 7 : 6.

<sup>c</sup> Major : minor ratio *ca.* 3 : 2.

<sup>d</sup> Major : minor ratio *ca.* 3 : 2, data from Ref. 5.

<sup>e</sup> Data from Ref. 8.

<sup>f</sup> Data from Ref. 9.

<sup>g</sup> Not measured owing to severe line broadening.

<sup>h</sup> Not assigned.

species}, and a 2.5% NOE for minor H-62 upon {7.58 ppm, 5 minor species H-7}. While two symmetry unrelated molecules reside in the asymmetric unit of crystalline TCfC-5e, the root mean square (RMS) difference for superimposition<sup>17</sup> of all non-hydrogen atoms was only 0.077 Å (i.e. both molecules are virtually identical).<sup>15</sup> The H-62...H-7 distances of 2.31 and 2.29 Å in the two solid-state molecules are commensurate with the above-mentioned NOE observations.

### Time-averaged <sup>3</sup>J(HH) coupling constants and conformational interconversion

We previously showed a pH dependence for the NMR observation of two species (major/minor) for the parent nefopam·HCl (**1**) dissolved in D<sub>2</sub>O (two species in acidic D<sub>2</sub>O, whereas a single-species time-averaged spectrum was recorded at neutral pH).<sup>3a,5</sup> The *ca.* 5 Hz doublet multiplicity found for all major and minor species *N*-methyl proton signals of **1**, **5** and **6** is typical of vicinal <sup>+</sup>NHCH<sub>3</sub> coupling, and thus indicates a slow exchange limit (SEL) kinetic regime for <sup>+</sup>*N*-configurational diastereomerization involving a prototropic shift/nitrogen inversion mechanism. Inspection of the vicinal coupling constant magnitudes in Table 1 shows time-averaged values for major/minor species of each epimer (**5** and **6**), and also for some other nefopam

structures. Since ring inversion for nefopam and derivatives has been shown to result in a sterically hindered (and hence energetically unfavourable) *endo* orientation for the phenyl ring,<sup>3b</sup> this may be ruled out as a cause. Therefore, it is reasonable to interpret time-averaged NMR spectral parameters for nefopam and derivatives in terms of rapid TCfC ⇌ BfC conformational interchange.<sup>3b</sup> In this diastereomerization, the sterically favoured *exo* disposition of the phenyl ring remains invariant while only the conformation of the —OCH<sub>2</sub>CH<sub>2</sub>NH(CH<sub>3</sub>)— fragment changes. Moreover, this process has been observed by x-ray crystallography of crystalline **3** (as mentioned earlier, statistically different ratios of BfC-**3** and TCfC-**3** occupancy factors were found for the same conformationally disordered data crystal as a function of data collection temperature).<sup>11</sup>

Molecular mechanics models were calculated for four species using the MMX<sup>18</sup> force field [TCfC-5e, BfC-5a, TCfC-5a, BfC-5e; corresponding sets of four were also made for the epimer (**6**) and parent **1**]. Two MMX models were calculated for **2** (TCfC-2, BfC-2) and a corresponding set was made for **3**. Vicinal H—C(or N)—C—H torsion angles in the molecular mechanics models are listed in Table 2. The MMX calculated models were in excellent agreement with the respective x-ray crystallographically determined geometries of nefopam and derivatives (e.g. TCfC-5e and BfC-6e).

Table 2. Vicinal H—C(or N)—C—H torsion angles in MMX molecular mechanics models of structures **1**, **2**, **3**, **5**, **6** and **8** involved in rapid conformational interchange

	H—C(or N)—C—H torsion angles (°)											
	31.41	31.42	32.41	32.42	41.51	41.52	42.51	42.52	51.61	51.62	52.61	52.62
Minor species (1S,5S)-1:												
TCfC-1a	46.1	-69.0	-72.3	172.6	-71.7		43.2		-77.3	32.6		
BfC-1e	172.3	58.2	54.4	-59.7	178.3		-66.2		-33.2	77.4		
Major species (1S,5R)-1:												
TCfC-1e	46.6	-69.7	-71.8	171.9		58.7		176.0			147.0	-98.7
BfC-1a	167.1	54.4	50.5	-62.1		-54.5		58.3			-158.7	-46.4
(1S)-2:												
TCfC-2	51.8	-65.3	-68.1	174.8	-67.0	50.0	48.5	165.5	-83.5	28.2	159.5	-88.7
BfC-2	159.1	43.7	40.4	-74.9	169.2	-73.3	-76.1	41.5	-17.8	94.2	-135.2	-23.2
(1S)-3:												
TCfC-3	46.8	-65.9	-72.6	174.7								
BfC-3	163.8	52.4	46.4	-64.8								
Minor species (1S,3R,5R)-5:												
TCfC-5e			-73.5	170.3		60.0		176.4			147.1	-99.1
BfC-5a			44.5	-66.5		-47.3		63.3			-166.6	-53.4
Major species (1S,3R,5S)-5:												
TCfC-5a			-73.3	171.1	-69.8		44.3		-77.9	31.8		
BfC-5e			52.0	-61.4	179.2		-66.4		-34.9	75.7		
Minor species (1S,3S,5S)-6:												
TCfC-6a	57.0	-56.1			-71.2		41.3		-77.3	32.8		
BfC-6e	177.6	63.3			178.4		-66.4		-34.9	75.9		
Major species (1S,3S,5R)-6:												
TCfC-6e	54.4	-60.8				68.0		-176.3			138.5	-107.1
BfC-6a	172.7	60.0				-52.9		59.9			-161.9	-49.0
Major species (1S,5S,6S)-8:												
<sup>4</sup> C <sub>1</sub> -8e	174.1	56.3	54.0	-63.7	-174.2		-56.4		175.6		-178.0 <sup>a</sup>	
<sup>1</sup> C <sub>4</sub> -8a	65.0	-50.4	-54.3	169.7	-76.9		38.4		75.4		-69.3 <sup>a</sup>	

<sup>a</sup> Torsion angle 1.61.

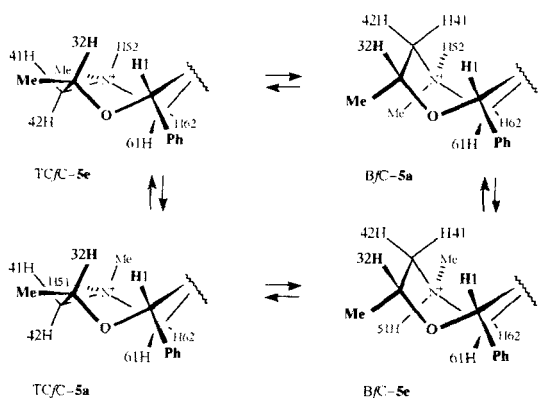


**Figure 1.** Twist-chair-(flattened chair)/boat-(flattened chair) conformational interconversion (horizontal pathways) and prototropic shift/nitrogen inversion configurational interchange (vertical pathways) for dissolution of crystalline (1*R*,3*S*,5*S*)/(1*S*,3*R*,5*R*)-TCfC-**5e** in CD<sub>2</sub>Cl<sub>2</sub>. Estimated partitioning: TCfC-**5e** 35%, TCfC-**5a** 35%, BfC-**5e** 20% and BfC-**5a** 10% (minimum estimated error ±5%).

For example, superimposition of all non-halogen heavy atoms of the TCfC-**5e** molecular mechanics model with the two independent TCfC-**5e** molecules in the crystal asymmetric unit gave relatively low RMS fit values of 0.081 and 0.092 Å.<sup>17</sup> Conformational BfC ⇌ TCfC interconversion inverts the synclinal (*gauche*) O-2-C-3-C-4-N-5 torsion angle sign (and exchanges the equatorial/axial substituent dispositions at ring-positions 3-5 (illustrated by TCfC-**5e** ⇌ BfC-**5a** and TCfC-**5a** ⇌ BfC-**5e**) (see Figs 1 and 2). <sup>+</sup>N-configurational interconversion is shown by BfC-**5a** ⇌ BfC-**5e** and TCfC-**5e** ⇌ TCfC-**5a** (see Figs 1 and 2).

Estimated vicinal coupling constants based on H-C(or N<sup>+</sup>)-C-H dihedral angles in the molecular mechanics models and weighted-average calculated values resulting from rapid TCfC ⇌ BfC conformational interchange are listed in Table 3. Hassnoot *et al.*'s<sup>19</sup> generalized Karplus<sup>13</sup> equation was used for coupling constants in the -OCH<sub>2</sub>CH<sub>2</sub>N- fragment.<sup>14</sup> Hassnoot *et al.*<sup>19</sup> showed that the relative orientation and electronegativity of X and Y substituents in -CH(X)CH(Y)- segments modified the Karplus

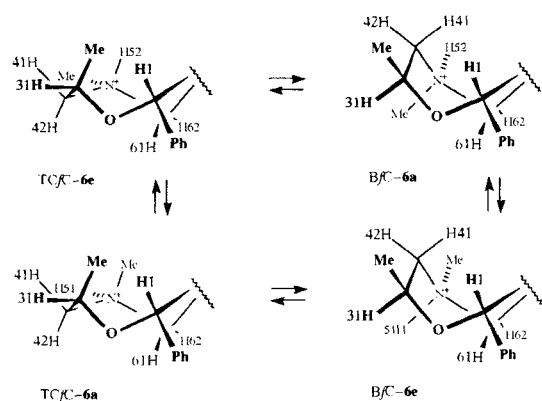
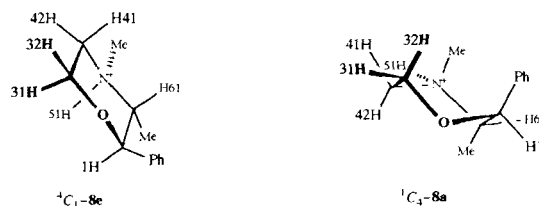


**Figure 2.** Twist-chair-(flattened chair)/boat-(flattened chair) conformational interconversion (horizontal pathways) and prototropic shift/nitrogen inversion configurational interchange (vertical pathways) for dissolution of crystalline (1*R*,3*R*,5*R*)/(1*S*,3*S*,5*S*)-BfC-**6e** in CD<sub>2</sub>Cl<sub>2</sub>. Estimated partitioning: TCfC-**6e** 5%, TCfC-**6a** 5%, BfC-**6e** 35% and BfC-**6a** 55% (minimum estimated error ±5%).

relationship for vicinal coupling constants. Other coupling constants were calculated using the dihedral angular dependence of H-N<sup>+</sup>-C-H coupling constants reported by Fraser *et al.*<sup>20</sup> Orientation and electronegativity effects of X and Y substituents in -NH(X)CH(Y)- segments have not been taken into consideration in this <sup>3</sup>J(HNCH) = 9.8 cos<sup>2</sup> θ - 1.8 cos θ relationship.<sup>20</sup>



Before calculation of <sup>3</sup>J(HH) values for each of the components in the rapid TCfC ⇌ BfC equilibrium, Hassnoot *et al.*'s generalized Karplus equation was used on a conformationally biased morpholine derivative, phendimetrazine mesylate<sup>3c</sup> (**8**) (the bitartrate salt is used therapeutically as an anorexic drug<sup>21</sup>). For the convenience of this work, the normal numbering system for 3,4-dimethyl-2-phenylmorpholine (**8**) was converted to that used for nefopam and derivatives. Four MMX models were made for **8** [<sup>4</sup>C<sub>1</sub>-**8e**, <sup>1</sup>C<sub>4</sub>-**8a**, <sup>4</sup>C<sub>1</sub>-**8a** and <sup>1</sup>C<sub>4</sub>-**8e**]. Two *N*-methyl diastereomers were observed for **8** in CD<sub>2</sub>Cl<sub>2</sub> solution in the ratio of 17:1.<sup>3c</sup> Each species exhibits a *ca.* 5 Hz doublet for the *N*-methyl protons, testifying to SEL kinetics for prototropic shift/nitrogen inversion.<sup>3c</sup> Torsion angles and calculated vicinal coupling constants for the -OCH<sub>2</sub>CH<sub>2</sub>N- and -OCH(Ph)CH(Me)N- fragments in MMX models <sup>4</sup>C<sub>1</sub>-**8e** and <sup>1</sup>C<sub>4</sub>-**8a** are listed in Tables 2 and 3. There is excellent agreement between experimental and calculated values using Hassnoot *et al.*'s method<sup>14</sup> [calculated <sup>4</sup>C<sub>1</sub>-**8e** values are 9.8 Hz <sup>3</sup>J(1,61), 11.3 Hz <sup>3</sup>J(31,41), 2.7 Hz <sup>3</sup>J(31,42), 4.2 Hz <sup>3</sup>J(32,41) and 1.1 Hz <sup>3</sup>J(32,42); the respective experimentally measured values are 9.7 (1), 11.6 (1), 2.2 (1), 4.5 (1) and 1.1 (1) Hz].<sup>3c</sup> Only one stereochemically relevant coupling constant was found<sup>3c</sup> for minor species **8** [10.2 (1) Hz <sup>3</sup>J(1,61) doublet found versus 9.7 Hz calculated<sup>14</sup> based on a 179.4° torsion angle in <sup>4</sup>C<sub>1</sub>-**8a**]. The calculated major species H-H-C-H coupling constants using Fraser *et al.*'s method<sup>20</sup> are 11.5 Hz <sup>3</sup>J(41,51), 2.0 Hz <sup>3</sup>J(42,51) and 11.5 Hz <sup>3</sup>J(51,61) for <sup>4</sup>C<sub>1</sub>-**8e**; the corresponding found values<sup>3c</sup> are 9.8 (1), 2.5 (1) and 9.0 (1) Hz. Although the quality of agreement is now slightly reduced (presumably since orientation and electronegativity effects are not calculated), application of Hassnoot *et al.*'s equation to H-N-C-H is even less satisfactory. Clearly, the overall congruence between experi-

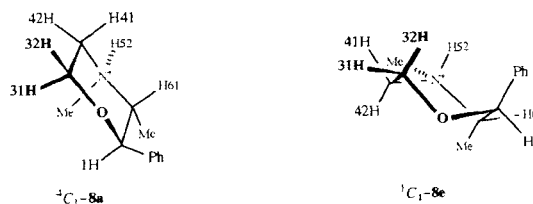


**Table 3. Vicinal  $^3J(\text{HH})$  coupling constants estimated from dihedral angles in MMX models of 1, 2, 3, 5, 6 and 8 and weighted-average calculated values resulting from rapid TCfC-BfC conformational interchange<sup>a</sup>**

	Estimated vicinal $^3J(\text{HH})$ coupling constants (Hz)											
	31,41	31,42	32,41	32,42	41,51	41,52	42,51	42,52	51,61	51,62	52,61	52,62
Minor species (1 <i>R</i> ,5 <i>R</i> )/(1 <i>S</i> ,5 <i>S</i> )-1 (based on weighted average calculated = TCfC-1 <i>a</i> :BfC-1 <i>e</i> = 1:3):												
TCfC-1 <i>a</i>	3.4	2.1	1.0	11.3	0.4	3.9			0.1	5.4		
BfC-1 <i>e</i>	11.3	2.4	4.2	1.5	11.6	0.9			5.4	0.1		
1:3 calc.	9.3	2.9	3.9	3.7	8.8	1.7			3.8	1.4		
Expt. <sup>b</sup>	10.8 (3)	3.2 (3)	3.4 (3)	3.0 (2)	7.7 (2)		2.7 (3)		2.9 (1)	<1		
Major species (1 <i>R</i> ,5 <i>S</i> )/(1 <i>S</i> ,5 <i>R</i> )-1 (based on weighted average calculated = TCfC-1 <i>e</i> :BfC-1 <i>a</i> = 1:19):												
TCfC-1 <i>e</i>	3.3	1.0	1.9	11.3		1.7		11.5			8.4	0.5
BfC-1 <i>a</i>	11.2	3.0	4.7	2.3		2.3		1.8			10.2	3.4
1:19 calc.	10.8	2.9	4.6	2.8		2.3		2.3			10.1	3.3
Expt. <sup>b</sup>	12.0 (2)	4.3 (3)	4.8 (2)	2.2 (3)		2.4 (2)		3.5 (3)			7.7 (1)	4.5 (2)
(1 <i>R</i> )/(1 <i>S</i> )-2 (based on weighted average calculated = TCfC-2:BfC-2 = 7:13):												
TCfC-2	2.5	2.6	1.3	11.3	0.8	2.9	3.1	10.9	0.1	6.0	10.3	0.0
BfC-2	10.8	4.5	6.4	0.4	11.2	0.3	0.1	4.1	7.2	0.2	6.2	6.6
7:13 calc.	8.1	3.6	4.4	4.2					4.6	2.2	8.7	3.6
Expt. <sup>c</sup>	8.1 (2)	5.1 (2)	3.9 (1)	3.9 (1)	<sup>d</sup>	<sup>d</sup>	<sup>d</sup>	<sup>d</sup>	3.3 (2)	2.6 (5)	8.9 (4)	3.9 (5)
(1 <i>R</i> )/(1 <i>S</i> )-3 (based on weighted average calculated = TCfC-3:BfC-3 = 1:19):												
TCfC-3	3.4	2.5	0.9	11.4								
BfC-3	11.2	3.2	5.6	1.0								
1:19 calc.	10.8	3.2	5.4	1.5								
Expt. <sup>e</sup>	12.8 (1)	3.8 (1)	4.3 (2)	<1								
Minor species (1 <i>R</i> ,3 <i>S</i> ,5 <i>S</i> )/(1 <i>S</i> ,3 <i>R</i> ,5 <i>R</i> )-5 (based on weighted average calculated = TCfC-5 <i>e</i> :BfC-5 <i>a</i> = 4:1):												
TCfC-5 <i>e</i>			1.5	10.1		1.6		11.6			8.4	0.5
BfC-5 <i>a</i>			5.5	1.1		3.3		1.6			11.0	2.4
4:1 calc.			2.3	8.3		1.9		9.6			8.9	0.9
Expt.			2.2 (1)	8.5 (1)		3.2 (1)		7.9 (2)			7.2 (1)	<1
Major species (1 <i>R</i> ,3 <i>S</i> ,5 <i>R</i> )/(1 <i>S</i> ,3 <i>R</i> ,5 <i>S</i> )-5 (based on weighted average calculated = TCfC-5 <i>a</i> :BfC-5 <i>e</i> = 6:4):												
TCfC-5 <i>a</i>			1.6	10.2		0.5		3.7	0.1	5.5		
BfC-5 <i>e</i>			4.6	1.5		11.6		0.9	5.1	0.2		
6:4 calc.			2.8	6.7		4.9		2.6	2.1	3.4		
Expt.			2.3 (1)	6.6 (1)		4.8 (4)		3.5 (1)	1.5 (1)	3.4 (1)		
Minor species (1 <i>R</i> ,3 <i>R</i> ,5 <i>R</i> )/(1 <i>S</i> ,3 <i>S</i> ,5 <i>S</i> )-6 (based on weighted average calculated = TCfC-6 <i>a</i> :BfC-6 <i>e</i> = 3:17):												
TCfC-6 <i>a</i>	1.9	1.7			0.4		1.8		0.1	5.4		
BfC-6 <i>e</i>	11.1	2.3			11.6		0.9		5.1	0.1		
3:17 calc.	9.7								4.4	0.9		
Expt.	10.8	<sup>d</sup>			<sup>d</sup>		<sup>d</sup>		3.0 (2)	<1		
Major species (1 <i>R</i> ,3 <i>R</i> ,5 <i>S</i> )/(1 <i>S</i> ,3 <i>S</i> ,5 <i>R</i> )-6 (based on weighted average calculated = TCfC-6 <i>e</i> :BfC-6 <i>a</i> = 1:19):												
TCfC-6 <i>e</i>	2.2	3.4				0.7		11.6			6.8	1.4
BfC-6 <i>a</i>	10.4	2.6				2.5		1.6			10.6	3.0
1:19 calc.	10.0	2.6				2.4		2.1			10.4	2.9
Expt.	12.1 (3)	4.6 (1)				2.1 (3)		2.7 (2)			7.8 (3)	5.1 (1)
Major species (1 <i>R</i> ,5 <i>R</i> ,6 <i>R</i> )/(1 <i>S</i> ,5 <i>S</i> ,6 <i>S</i> )-8 (based on weighted average calculated = <sup>4</sup> C <sub>1</sub> -8 <i>e</i> : <sup>1</sup> C <sub>4</sub> -8 <i>a</i> = 19:1):												
<sup>4</sup> C <sub>1</sub> -8 <i>e</i>	11.3	2.7	4.2	1.1	11.5		2.0		11.5		9.8 <sup>f</sup>	
<sup>1</sup> C <sub>4</sub> -8 <i>a</i>	1.0	4.8	3.0	10.3	0.1		4.6		0.2		0.9 <sup>f</sup>	
19:1 calc.	10.8	2.8	4.1	1.6	10.9		2.1		10.9		9.4	
Expt.	11.6 (1)	2.2 (1)	4.5 (1)	1.1 (1)	9.8 (1)		2.5 (1)		9.0 (1)		9.7 (1) <sup>f</sup>	

<sup>a</sup> Coupling constants  $^3J(31,41)$ ,  $^3J(31,42)$ ,  $^3J(32,41)$  and  $^3J(32,42)$  estimated using Hassnoot *et al.*'s generalized Karplus relationship,<sup>14</sup> all others based on the H—N—C—H angular relationship of Fraser *et al.*,<sup>20</sup> estimated standard deviation (esd) for last digit of experimental *J*-value given in parentheses.

<sup>b</sup> Data from Ref. 5.

<sup>c</sup> Data from Ref. 8.

<sup>d</sup> Not measured.

<sup>e</sup> Data from Ref. 3c.

<sup>f</sup> Coupling constant 1.61.

mental and calculated coupling constants of major species **8** is consistent with a bias for a <sup>4</sup>C<sub>1</sub>-8*e* chair conformation having three equatorially disposed substituents. A crude estimation of *ca.* 19:1 for the respective chair-chair interconverting <sup>4</sup>C<sub>1</sub>-8*e* and <sup>1</sup>C<sub>4</sub>-8*a* isomers (minimum estimated error  $\pm 5\%$ ) was calculated by weighted averages of the eight stereochemically relevant vicinal coupling constants listed for individual conformers in Table 3.

Dissolution of crystalline BfC-1*e*, TCfC-5*e* or BfC-6*e* gives rise to an epimerization affording two diastereomers differing in configuration at the stereolabile protonated nitrogen. Each *N*-methyl diastereomer undergoes a diastereomerization into TCfC and BfC conformations, i.e. a total of four interconverting diastereomers (see Figs 1 and 2 for the case of TCfC-5*e* and BfC-6*e*). Similarly, dissolution of crystalline BfC-1*e* or the disordered BfC-3/TCfC-3 crystals also gives

**Table 4. Quantitative estimation of boat-(flattened chair) (BfC) and twist-chair-(flattened chair) (TCfC) conformations on dissolution in CD<sub>2</sub>Cl<sub>2</sub> of crystalline nefopam hydrochloride (1), *N*-desmethylnefopam hydrochloride (2), nefopam methiodide (3) and the 3-methylnefopam hydrochloride epimers (5 and 6)<sup>a</sup>**

Solid-state conformation	Solution-state conformations			
	BfC-eq. <i>N</i> -methyl	BfC-ax. <i>N</i> -methyl	TCfC-eq. <i>N</i> -methyl	TCfC-ax. <i>N</i> -methyl
BfC-1e	30	55	5	10
TCfC-5e	20	10	35	35
BfC-6e	35	55	5	5
		BfC		TCfC
BfC-2		65		35
BfC-3/TCfC-3 (disorder 56:44)		95		5

<sup>a</sup> Percentage estimated from major:minor isomer ratios in Table 1 and weighted average calculated coupling constants in Table 3, minimum estimated error  $\pm 5$ .

rise to the same diastereomerization into TCfC and BfC conformations. In a manner analogous to that described above for phendimetrazine, weighted average coupling constants calculated from corresponding values of the individual structures listed in Table 3 enable us to estimate the amounts of TCfC and BfC forms for each species observed in the NMR spectrum (see Table 4).

The following semiquantitative general conclusions may be drawn from the data in Table 4. Both the BfC and TCfC conformations are present in significant amounts in a CD<sub>2</sub>Cl<sub>2</sub> solution of *N*-desmethylnefopam·HCl (BfC-2:TCfC-2 ratio  $\approx 2:1$ ). Mono-*N*-methylation of the 2,5-benzoxazocine ring [i.e. nefopam·HCl (1)] increases the total amount of BfC conformers in solution (from *ca.* 67% to *ca.* 85%). The axial *N*-methyl diastereomer of each conformational type appears to be favoured over the corresponding equatorial epimer [i.e. BfC-1a > BfC-1e and TCfC-1a > TCfC-1e]. It is likely that this situation arises from differences in solute-solvent interactions, since molecular mechanics shows the axial epimer in each conformational series to be *ca.* 3.8 kJ higher in energy.<sup>3b</sup> A second *N*-methylation [i.e. nefopam methiodide quaternary ammonium salt (3)] further increases the quantity of BfC conformer in solution [*ca.*  $\geq 95\%$ ]. Little or no change in the amount of BfC solution-state conformations (*ca.* 90%) relative to the parent nefopam·HCl (1) was found when the second methyl replaced the *trans*-to-phenyl proton on C-3 (i.e. epimer 6). The *trans*-to-phenyl *C*-methyl resides in an equatorial position in the two solution-state BfC conformations of 6. *cis*-1,3-Diaxial dimethyl interactions in the C-3 epimer appear to reduce the amount of TCfC-6a relative to TCfC-6e (*ca.* 5% each) compared with TCfC-1a:TCfC-1e (*ca.* 10% and *ca.* 5%, respectively). The 2,5-benzoxazocine conformational preference is markedly altered to TCfC (*ca.* 70% total) when a second methyl group replaces the *cis*-to-phenyl proton on C-3 (i.e. epimer 5). The *cis*-to-phenyl *C*-methyl also resides in an equatorial position in the two solution-state TCfC conformations of 5. Again, *cis*-1,3-diaxial dimethyl non-bonding interactions appear to reduce the amount of BfC-5a relative to BfC-5e (*ca.* 10% and *ca.* 20%, respectively). There does not appear to be a preferred *N*-methyl orientation for the TCfC conformation as judged by the equal

amounts for TCfC-5a and TCfC-5e isomers (*ca.* 35% each).

The line widths in the <sup>1</sup>H NMR spectra of nefopam hydrochloride and derivatives undergoing BfC-TCfC exchange in CD<sub>2</sub>Cl<sub>2</sub> solution are narrow for some species and broadened for others. Thus, the eight-membered ring conformational interchange occurs at different kinetic rate regimes on the NMR time-scale. For example, fast exchange limit (FEL) narrow line widths but time-averaged spectral parameters were observed for major and minor species of *cis*-to-phenyl 3-methylnefopam·HCl epimer 5, major species of *trans*-to-phenyl 3-methylnefopam·HCl epimer 6 and the major species of parent nefopam·HCl (1). Fast magnetic site-exchange broadened <sup>1</sup>H NMR line widths were found for the *trans*-to-phenyl 3-methylnefopam·HCl epimer 6 minor species, minor species of parent nefopam·HCl (1), *N*-desmethylnefopam·HCl (2) and nefopam methiodide (3).

#### Time-averaged NOE intensity enhancements and conformational interconversion

BfC-TCfC conformational changes result in weighted time-averages for all NMR spectral parameters including chemical shifts and nuclear Overhauser effects. NOE intensity enhancements are consistent with the major component TCfC-5e structure proposed for the *cis*-to-phenyl 3-methylnefopam·HCl minor species (TCfC-5e  $\rightleftharpoons$  BfC-5a, *ca.* 4:1). For example, axial H-42 in TCfC-5e is closer to its transannular neighbour H-61 than to H-62 (see Fig. 1) {average distances in the two independent TCfC-5e molecules of the crystal are 2.48 (2) Å [H-42...H-61], and 3.40 (2) Å [H-42...H-62]}. NOE intensity enhancements are consistent with this arrangement: a 1.4% NOE for  $\delta$  5.15 [H-61] upon {H-42, 2.82 ppm}. In addition, H-32 has *cis*-1,3-diaxial type interactions with both H-1 and H-52 in TCfC-5e {average distances in crystalline TCfC-5e are 2.38 (1) Å [H-32...H-1], and 2.45 (2) Å [H-32...H-52]}. A 1.6% NOE for  $\delta$  12.60 [H-52] upon {H-32, 4.33 ppm} and a 1.2% NOE for  $\delta$  4.33 [H-32] upon {H-52, 12.60 ppm} are in agreement with the TCfC-5e conformation. However, a 2.24 Å H-32...H-1 non-bonding distance

in *BfC-5a* shows that this close contact is not unique to only one of the two interconverting diastereomers. Thus, the 5.9% NOE for  $\delta$  4.33 [H-32] upon {H-1, 5.89 ppm} and the 6.6% NOE for  $\delta$  5.89 [H-1] upon {H-32, 4.33 ppm} is consistent with the H-32 *cis*-to-H-1 arrangement found for both *TCfC-5e* and *BfC-5a*.

Nuclear Overhauser effect measurements are also consistent with an axial assignment of  $\delta$  2.56 *N*-methyl in the preponderant component *TCfC-5a* structure proposed for the *cis*-to-phenyl 3-methylnepomam·HCl major species (*TCfC-5a*  $\rightleftharpoons$  *BfC-5e*, *ca.* 6:4). A 1.8% NOE for  $\delta$  4.14 [H-32] upon {H-132  $CH_3N$ , 2.56 ppm} is in agreement with the *cis*-1,3-diaxial type interaction between H-32 and the  $NCH_3$  protons in *TCfC-5a* (2.26 Å [H-32  $\cdots$   $CH_3N$ , minimum distance]). However, a 2.9% NOE for  $\delta$  4.14 [H-32] upon {H-1, 5.82 ppm} and 4.3% NOE for  $\delta$  5.82 [H-1] upon {H-32, 4.14 ppm} is not unique to only one of the two interconverting eight-membered ring conformations since the H-32  $\cdots$  H-1 non-bonding distance is 2.33 Å in *TCfC-5a* and 2.29 Å in *BfC-5e*. While these NOE observations may not be unique for a particular conformation, they do serve the important purpose of unequivocally assigning  $\delta$  5.82 and 5.89 singlet H-1 resonances to the respective major and minor species of **5**.

Similarly, the *trans*-to-phenyl *C*-methyl group in 3-methylnepomam·HCl epimer **6** is now in proper juxtaposition for NOE phenomena involving H-1 and *C-CH<sub>3</sub>* protons (see Fig. 2). Again, this situation permitted the unequivocal assignment of  $\delta$  5.98 and 5.94 singlet H-1 resonances to the respective major and minor species of **6**. Thus, irradiation of the  $\delta$  5.98 H-1 singlet afforded a 1.4% NOE enhancement to nearby  $\delta$  1.44 H-202 ( $CCH_3$ ) of the major species, and a 2.3% NOE for  $\delta$  5.98 [H-1] upon {H-202  $CCH_3$ , 1.44 ppm}, while irradiation of the minor species H-202  $CCH_3$   $\delta$  1.41 resonance resulted in a 5.5% NOE for  $\delta$  5.94 [H-1]. In addition, NOE intensity enhancements are in agreement with the axial *N*-methyl orientation for the predominant *BfC-6a* structure of the major species (*TCfC-6e*  $\rightleftharpoons$  *BfC-6a*, *ca.* 1:19). A 2.3% NOE for  $\delta$  4.70 [H-31] upon {H-131  $CH_3N$ , 2.99 ppm} is in accord with the 2.01 Å H-31  $\cdots$   $CH_3N$  minimum distance in model *BfC-6a*.

### <sup>13</sup>C NMR spectroscopy

Similarly to the other NMR spectral parameters discussed above, the <sup>13</sup>C chemical shift values are at the slow exchange limit for prototropic shift/nitrogen inversion, and at the fast exchange limit for eight-membered ring conformational interchange. Table 1 shows that even in this case, <sup>13</sup>C chemical shift values portray stereochemical information concerning the preponderant conformational forms for each of the major and minor species of **5** and **6**. The *C*-methyl and *C*-1 carbons are characteristically more strongly shielded by an average of *ca.* 3.8 and *ca.* 6.9 ppm respectively, in both species of **6** versus corresponding resonances in **5**. This is due to the so-called 'γ-effect'<sup>22</sup> resulting from the  $CCH_3 \cdots H-1$  *cis*-1,3-diaxial interaction in **6** (compare Fig. 1 and 2). The *TCfC-5a* and *TCfC-5e* isomers are the major components of the respective major and

minor species for **5**, and together they account for *ca.* 70% of the population. The *N*-methyl carbon in the major species is shifted 4.96 ppm upfield in accord with its proposed axial orientation in *TCfC-5a* relative to an equatorial disposition in *TCfC-5e*, although the 0.07 ppm shift upfield for the corresponding *C*-3 nucleus γ to  $NCH_3$  is negligible. Similarly, the *BfC-6a* and *BfC-6e* isomers are the major components of the respective major and minor species for **6**, and together they account for *ca.* 90% of the population. The *N*-methyl carbon in the major species is shifted 2.12 ppm upfield in accord with its axial orientation in *TCfC-6a* relative to an equatorial disposition in *TCfC-6e*, while the corresponding *C*-3 nucleus γ to  $NCH_3$  is shifted 2.09 ppm shift upfield. The magnitudes of the 'γ-effect' upfield shifts appear to be relatively small compared to more conformationally biased molecules. For example, the  $NCH_3$ , *C*-6 (β to the methyl) and *C*-1,3 (γ to the methyl) in the minor <sup>1</sup>*C*<sub>4</sub>-**8a** axial *N*-methyl diastereomer were characteristically more strongly shielded ( $\Delta\delta$  9.17, 4.40, 4.55 and 5.05 ppm, respectively) *vis-à-vis* corresponding carbon atoms in the major <sup>4</sup>*C*<sub>1</sub>-**8e** equatorial *N*-methyl diastereomer.<sup>3c</sup>

## EXPERIMENTAL

### Compounds

(1*R*,3*S*,5*R*)/(1*S*,3*R*,5*S*)- and (1*R*,3*R*,5*R*)/(1*S*,3*S*,5*S*)-3-methylnepomam hydrochloride (**5** and **6**). Purified thionyl chloride (6.5 ml, 90 mmol) was added slowly to a solution of *o*-benzoylbenzoic acid (6.8 g, 30 mmol) in toluene (40 ml), and then heated for 2 h at 90 °C, followed by vaporation *in vacuo* to yield the crude acid chloride as an oil. (±)-*N*-Methyl-1-aminopropan-2-ol (2.67 g, 30 mmol) and triethylamine (5.6 ml, 40 mmol) were added to a solution of crude *o*-benzoylbenzoyl chloride (7.33 g, 30 mmol) in toluene (30 ml), then refluxed with stirring overnight and cooled. After filtration, the filtrate was evaporated *in vacuo* to yield an oil. The oil was dissolved in chloroform, washed with 10% HCl, then with saturated NaCl solution, dried over anhydrous  $MgSO_4$ , filtered, evaporated *in vacuo* to dryness and purified by silica gel column chromatography to yield 4.1 g (48% yield) of the intermediate *cis*-/*trans*-amides.

A solution of the *cis*-/*trans*-amides (3.9 g, 13 mmol) in anhydrous tetrahydrofuran (30 ml) was added dropwise to a stirred suspension of lithium aluminium hydride (1.5 g, 40 mmol) in anhydrous tetrahydrofuran, refluxed overnight, cooled and then carefully treated consecutively with water (1.5 ml), 6 M NaOH solution (1.5 ml) and water (4.5 ml). The white solid was filtered off and washed with warm tetrahydrofuran. The combined filtrates were evaporated *in vacuo* and the resulting oil was dissolved in dimethyl ether and then washed three times with dilute HCl. The combined aqueous layers were treated with solid KOH until basic and extracted three times with  $CHCl_3$ . The combined organic layers were dried over anhydrous  $MgSO_4$ , filtered and evaporated *in vacuo* to dryness to yield 2.8 g (77% yield) of

the intermediate aminodiol diastereomeric mixture (ca. 52:48 ratio by  $^1\text{H}$  NMR).

A solution of aminodiols (2.8 g, 9.8 mmol) and *p*-toluenesulphonic acid monohydrate (2.9 g, 15 mmol) in toluene (40 ml) was refluxed overnight with a Dean-Stark trap, cooled, treated with excess 6 M NaOH solution and the organic layer was separated. After extraction of the aqueous layer three times with  $\text{CHCl}_3$ , the combined organic layers were dried over anhydrous  $\text{MgSO}_4$ , filtered, and then evaporated *in vacuo* to dryness to give 1.85 g (70% yield) of (1*R*,3*R*)/(1*S*,3*S*)- and (1*R*,3*S*)/(1*S*,3*R*)-3-methylnepfam free base diastereomeric mixture (1:2 ratio by  $^1\text{H}$  NMR). The free base diastereomeric mixture was separated by silica gel column chromatography to afford two fractions,  $^1\text{H}$  NMR ( $\text{CDCl}_3$ ) of first fraction [(1*R*,3*S*)/(1*S*,3*R*)-3-methylnepfam free base, stereochemistry determined by x-ray crystallography of resulting HCl salt]:  $\delta$  5.79 s, H-1; 4.00 ddq, H-32; 2.59 dd, H-41; 2.51 dd, H-42; 4.83 d, H-61; 3.54 d, H-62; 2.41 s, H-13  $\text{NCH}_3$ ; and 1.27 d, H-201  $\text{CCH}_3$ ;  $J(\text{HH})$  (Hz) 6.5 (1) [32,201]; 1.5 (1) [32,41]; 7.8 (1) [32,42]; -13.3 (6) [41,42]; and -13.2 (1) [61,62]. Second fraction [(1*R*,3*R*)/(1*S*,3*S*)-3-methylnepfam free base, stereochemistry determined by x-ray crystallography of resulting HCl salt]:  $\delta$  6.05 s, H-1; 4.13 ddq, H-31, 2.73 dd, H-41; 2.50 dd, H-42; 4.60 d, H-61; 3.86 d, H-62; 2.39 s, H-13  $\text{NCH}_3$ ; and 1.19 d, H-202  $\text{CCH}_3$ ;  $J(\text{HH})$  (Hz) 6.6 (1) [31,202]; 9.1 (1) [31,41]; 2.3 (1) [31,42]; -14.6 (1) [41,42]; and -13.9 (1) [61,62].

The individual free bases were dissolved in acetone, treated with ethereal HCl until acidic to pH paper, and the resulting solids (**5** or **6**) were filtered. Crude (1*R*,3*S*)/(1*S*,3*R*)-3-methylnepfam hydrochloride (**5**) (360 mg) was dissolved in absolute ethanol, and on vapour diffusion of acetone yielded 253 mg of clear, colourless, crystalline prisms, belonging to the monoclinic space group  $P2_1/c$ , m.p. 174.0–174.5 °C (decomp.) (uncorrected).<sup>15</sup> Similarly, crude (1*R*,3*R*)/(1*S*,3*S*)-3-methylnepfam hydrochloride (**6**) (160 mg) yielded 103 mg of clear, colourless, crystalline needles, belonging to the orthorhombic space group  $P2_12_12_1$ , m.p. 195.5–196.0 °C (decomp.) (uncorrected).<sup>15</sup> Elemental analyses were in accord with the proposed empirical formulae, and x-ray crystallography showed **5** and **6** to have  $\text{TCfC-5e}$  and  $\text{BfC-6e}$  structures, respectively.<sup>15</sup>  $^1\text{H}$  and  $^{13}\text{C}$  NMR

aliphatic spectral parameters of **5** and **6** are listed in Table 1.

### Spectra

$^1\text{H}$  and  $^{13}\text{C}$  NMR spectra [4.7, 7.05 and 9.4 T,  $\text{CD}_2\text{Cl}_2$  (for the HCl salt),  $\text{CDCl}_3$  (for the free base), sealed 5 mm sample tube, 298 K] were obtained at 200.1, 300.1 and 400.1 MHz for  $^1\text{H}$  and at 50.3, and 75.5 MHz for  $^{13}\text{C}$  on Bruker WP-200-SY, AM-300 and AM-400 Fourier transform spectrometers. The deuterated solvent was used as an internal lock, and the residual protio  $\text{CDHCl}_2$  solvent was used as an internal secondary reference for spectra of the HCl salt ( $\delta_{\text{H}}$  5.32 and  $\delta_{\text{C}}$  53.8 relative to tetramethylsilane). Tetramethylsilane was used as an internal reference for spectra of the free base. Standard Bruker microprograms were used for the DEPT (90° and 135° pulse angles), difference NOE and XHCORR experiments. Blunt's<sup>14</sup> HYPERCARD stack for Hassnoot *et al.*'s<sup>19</sup> generalized Karplus equation was used to calculate coupling constants for the  $-\text{OCH}_2\text{CH}_2\text{N}-$  fragment.

### Molecular mechanics

The minimized energy geometries of the molecular mechanics calculated model compounds were determined using the Macintosh-II version of the PCMODEL/MMX 4.25 program,<sup>18</sup> and were performed on a Macintosh SE-30 computer equipped with a RasterOps 264/SE colour board and RGB colour monitor. MMX is an enhanced version of Allinger's MM2 program<sup>23</sup> with MMPI  $\pi$ -subroutines<sup>24</sup> incorporated for localized  $\pi$ -electron systems.

### Acknowledgements

Dr Michael A. Bernstein (Merck Frosst Centre for Therapeutic Research, Montreal) and Dr Dagfin Aksnes (University of Bergen, Norway) and thanked for enabling us to acquire NMR data at 7.05 and 9.4 T during visits to their laboratories. Gratitude is expressed to the Kreitman Family Endowment Fund, Ben-Gurion University of the Negev, for the purchase of a Bruker WP-200-SY FT-NMR spectrometer.

### REFERENCES

1. S. Budavari (Ed.), *The Merck Index*, 11th edn, p. 1018 and references cited therein. Merck, Rahway, NJ (1989).
2. M. W. Klohs, M. D. Draper, F. J. Patracek, K. H. Ginzl and O. N. Ré, *Arzneim. Forsch. (Drug Res.)* **22**, 13 (1972).
3. (a) R. Glaser, S. Cohen, D. Donnell and I. Agranat, *J. Pharm. Sci.* **75**, 772 (1986); (b) R. Glaser, G. Frenking, G. H. Loew, D. Donnell, S. Cohen and I. Agranat, *J. Chem. Soc., Perkin Trans. 2* 113 (1989); (c) R. Glaser, *Magn. Reson. Chem.* **27**, 1142 (1989).
4. L. K. Hansen, A. Hordvik and A. J. Aasen, *Acta Chem. Scand.* **38**, 327 (1984).
5. R. Glaser, G. Frenking, G. H. Loew, D. Donnell and I. Agranat, *New J. Chem.* **12**, 953 (1988).
6. K. Mislow and J. Siegel, *J. Am. Chem. Soc.* **107**, 3319 (1984).
7. G. L. Closs, *J. Am. Chem. Soc.* **81**, 5456 (1959).
8. R. Glaser, S. Geresh, J. Blumenfeld, D. Donnell, N. Sugisaka, M. Drouin and A. Michel, *J. Pharm. Sci.* **82**, 276 (1993).
9. R. Glaser, A. Peleg and S. Geresh, *Magn. Reson. Chem.* **28**, 389 (1990).
10. R. Glaser, A. Michel and M. Drouin, *Can. J. Chem.* **68**, 1128 (1990).
11. R. Glaser, A. Michel and M. Drouin, unpublished results.
12. J. B. Bremner, E. J. Browne, P. E. Davis, C. L. Raston and A. H. White, *Aust. J. Chem.* **33**, 1323 (1980).
13. (a) M. Karplus, *J. Chem. Phys.* **30**, 11 (1959); (b) M. Karplus, *J. Am. Chem. Soc.* **85**, 2870 (1963).
14. J. W. Blunt, *Altona's Generalized Karplus Equation (HYPERCARD Stack for Macintosh Computers)*. Department of Chemistry, University of Canterbury, Canterbury, New Zealand (1988).
15. R. Glaser, J. Blumenfeld, S. Geresh, D. Donnell, J. H. Rosland,

- K. Hole and K. Maartmann-Moe, *J. Pharm. Sci.* in press.
16. R. K. Harris, *Nuclear Magnetic Resonance Spectroscopy*, pp. 55–57. Pitman, London (1983).
  17. A. Sundin, *MACMIMIC 2.0 Program*. InStar Software, Lund (1991).
  18. *PCMODEL 4.25/MMX for Macintosh-II Computers*. Serena Software, Bloomington, IN (1990).
  19. C. A. Hassnoot, F. A. A. M. de Leeuw and C. Altona, *Tetrahedron* **36**, 2783 (1980).
  20. R. R. Fraser, R. N. Renaud, J. K. Saunders and Y. Y. Wigfield, *Can. J. Chem.* **51**, 2433 (1973).
  21. S. Budavari (Ed.), *The Merck Index*, 11th edn, p. 1146. Merck, Rahway, NJ (1989).
  22. D. K. Dalling and D. M. Grant, *J. Am. Chem. Soc.* **96**, 1827 (1974), and references cited therein.
  23. N. L. Allinger, *J. Am. Chem. Soc.* **99**, 8127 (1977).
  24. N. L. Allinger and J. T. Sprague, *J. Am. Chem. Soc.* **95**, 3893 (1973).